LA-UR-99-5532
Approved for public release; distribution is unlimited.

Title: **Mechanical properties and microstructure in low-activation martensitic steels F82H and Optimax after 800-MeV proton irradiation**

Author(s): Y. Dai, S.A. Maloy, G.S. Bauer, W.F. Sommer

Submitted to:

ELSEVIER

Journal of Nuclear Materials 283–287 (2000) 513–517

journal of nuclear materials

www.elsevier.nl/locate/jnucmat

Mechanical properties and microstructure in low-activation martensitic steels F82H and Optimax after 800-MeV proton irradiation

Y. Dai [a,*], S.A. Maloy [b], G.S. Bauer [a], W.F. Sommer [b]

[a] *Spallation Source Division, Paul Scherrer Institut, CH-5232 Villigen PSI, Switzerland*
[b] *APT/TPO, MS H809, Los Alamos National Laboratory, NM 87545, USA*

Abstract

Low-activation martensitic steels, F82H (mod.) and Optimax-A, have been irradiated with 800-MeV protons up to 5.9 dpa. The tensile properties and microstructure have been studied. The results show that radiation hardening increases continuously with irradiation dose. F82H has lesser irradiation hardening as compared to Optimax-A in the present work and DIN1.4926 from a previous study. The irradiation embrittlement effects are evident in the materials since the uniform elongation is reduced sharply to less than 2%. However, all the irradiated samples ruptured in a ductile-fracture mode. Defect clusters have been observed. The size and the density of defect clusters increase with the irradiation dose. Precipitates are amorphous after irradiation.

1. Introduction

For high-power ($\geqslant 1$ MW) spallation neutron sources, e.g. the European Spallation Source (ESS) and accelerator-driven systems (ADS), the beam window of the liquid-metal targets will be subjected to high radiation and thermal mechanical loads. Both austenitic and martensitic steels are tentative candidate materials for the containers of liquid–metal targets. As compared to austenitic steels, martensitic are stronger and have better thermal mechanical properties. The main limitation for conventional martensitic steels, e.g. T91 and HT9, is that their ductile–brittle transition temperature (DBTT) increases significantly after irradiation at temperatures below about 370°C [1]. However, this limitation could be overcome because the so-called low-activation martensitic steels developed recently by the fusion materials program, e.g. F82H and 9Cr2WVTa (ORNL Ht. 3791), show a much lower shift of DBTT after irradiation to several dpa with neutrons [2,3]. For this reason, the low-activation martensitic steels have been included in irradiation programs oriented for spallation targets [4,5]. The present paper will present the results of two kinds of low-activation steels, F82H and Optimax-A, irradiated with 800-MeV protons.

2. Experimental

Materials of both F82H and Optimax were obtained from the fusion materials group (PIREX) of EPFL, Switzerland. The F82H material was cut from a 15-mm thick plate (IEA Heat 9741). The nominal composition is: Fe + 7.7 Cr, 0.16 Mn, 0.16 V, 1.95 W, 0.02 Ta, 0.11 Si and 0.09 C in wt%. The plate was normalized at 1040°C for 38 min and tempered at 750°C for 1 h [6]. The Optimax-A material was developed by the PIREX group [7]. Its composition is: Fe + 9.0 Cr, 0.5 Mn, 0.18 V, 2.0 W, 0.09 Ta, 0.09 Si and 0.09 C in wt%. The material used in this work was cut from an 8-mm thick plate which was normalized at 1030°C for 30 min and tempered at 750°C for 1 h.

Miniature-type tensile samples were used in the present study. The samples were 0.25- or 0.75-mm thick, 5-mm long and 1.2-mm wide in gauge area. A total of 48

* Corresponding author. Tel.: +41-56 310 41 71; fax: +41-56 310 31 31.
E-mail address: yong.dai@psi.ch (Y. Dai).

0022-3115/00/$ - see front matter
PII: S0022-3115(00)00267-1

F82H and 24 Optimax tensile samples were irradiated with other samples of APT materials irradiation program at the Los Alamos Neutron Science Center (LANSCE) [4]. The samples were placed at two different positions, Insert 17A and Insert 18C. Samples in Insert 17A were irradiated mainly with high-intensity protons. Insert 18C is located after a tungsten target. Therefore, the samples in Insert 18C were irradiated with a much lower proton intensity as well as a much higher neutron intensity. The irradiation dose was determined starting with a calculation of proton and neutron fluences using the Los Alamos high-energy transport (LAHET) code. This initial calculated fluence was used along with the gamma counts on dosimetry foils placed alongside the specimens. A computer program called STAYSL2 determined the best proton and neutron fluences to match the gamma measurements made on the activation foils. The dpa cross-sections determined by the LAHET code were used to determine the dose for each specimen. The samples were packed in stainless steel envelopes with thickness ranging from 0.75 to 2.5 mm, which were cooled with H_2O at about 30°C during the irradiation. The irradiation temperature of the samples is between 30 to 100°C.

Tensile tests were performed on a 2-kN MTS mechanical test machine equipped with a video-extensometer so that the displacement was measured directly from the gauge area. The tests were performed at room temperature (22°C) with a strain rate of about 10^{-3} s^{-1}. Each tensile test was run until the sample failed. Most of the samples were then observed with scanning electron microscopy (SEM) to identify their fracture mode.

Transmission electron microscopy (TEM) investigation of the microstructure was performed with a JEOL 2010-type microscope equipped with an EDX analysis system. The most often used image conditions were bright field (BF) and weak beam–dark field (WBDF) at (g, $4g$) or (g, $6g$), $g = 110$.

3. Results

3.1. Tensile tests

Eight F82H and three Optimax irradiated specimens, together with a number of control specimens, have been tested. The irradiation doses for F82H samples are in the range of 0.5–5.9 dpa and for Optimax samples are 0.8, 1.4 and 4.7 dpa. The tensile stress–strain curves for the two kinds of materials are presented in Fig. 1. It can be seen that the behavior of the two materials looks very similar after irradiation: (a) both the yield stress and the ultimate tensile strength increase with irradiation dose; (b) the yield point is followed immediately by the necking point which, therefore, gives a very small uniform elongation. The results are summarized and given as Fig. 2(a) for the yield stress at 0.2% offset and the ultimate tensile strength, and Fig. 2(b) for uniform elongation and the total elongation vs irradiation dose. In Fig. 2(a), as the yield stresses of irradiated samples are very close to the ultimate tensile strengths, symbols are overlapped. In Fig. 2(b), the reduction in area deduced from SEM micrographs is also illustrated.

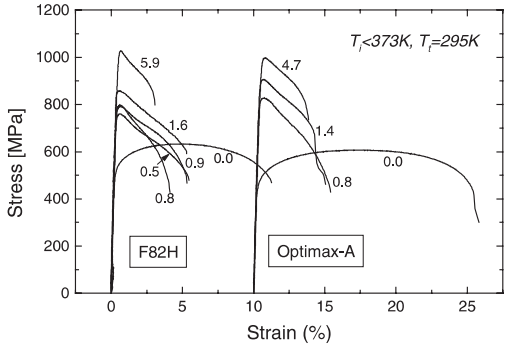

Fig. 1. Tensile test stress–strain curves of F82H and Optimax-A irradiated with 800-MeV protons at temperatures below 100°C and tested at room temperature. The dpa number of each curve is indicated.

3.2. SEM observation

SEM observation shows that the samples of F82H and Optimax have the same fracture mode in the dose

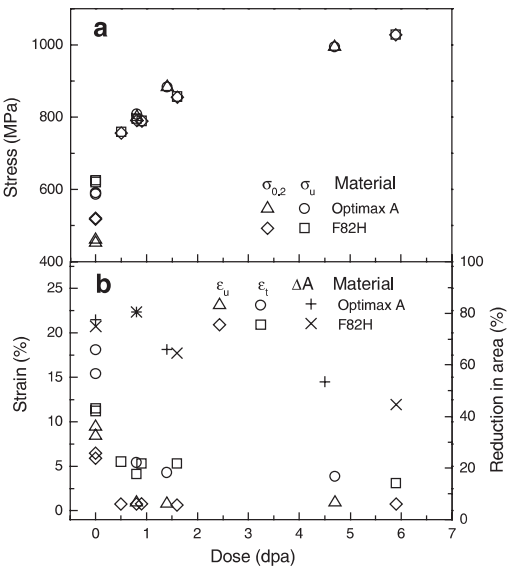

Fig. 2. Plots of (a) yield stress and ultimate tensile strength, and (b) uniform elongation, total elongation and reduction in area change with irradiation dose.

range examined. Irradiation embrittlement effects are illustrated by a decrease in the reduction of area with an increase in dose, as shown in Fig. 3. However, all the samples ruptured in a ductile-fracture mode. Fig. 4 shows the micrographs from unirradiated and highest dose samples for F82H, (a) and (b), and for Optimax-A, (c) and (d), respectively.

3.3. TEM investigation

The microstructure analysis shows that for the as-received materials, both F82H and Optimax-A have typical martensite lath structures. The precipitates are usually $M_{23}C_6$-type and rich in Cr (40–60 at.%), Fe (40–50 at.%) and W (2–5 at.%). The precipitates in F82H are mostly elongated and located at the lath boundaries. There are some relatively round and large ones in the matrix, see Fig. 5(a). Optimax-A has a much more round shape and larger precipitates in both matrix and lath boundaries, see Fig. 5(b). After irradiation, there are no evident changes noticed in precipitate distribution and compositions (analyzed by EDX). However, the precipitates become amorphous after irradiation, as illustrated by the ring diffraction patterns in Figs. 5(c) and (d) for F82H and Optimax-A, respectively.

The main feature of the change in microstructure induced by radiation damage is the appearance of small defect clusters. This is observed in all six irradiated samples investigated, which cover a dose range from 0.8 to 5.9 dpa. Fig. 6 demonstrates the situation in these six samples. It can be seen that the small defect clusters become denser and larger with increasing irradiation dose. The defect cluster size and density are given in Table 1. As the thickness of the thin foils was deduced from the number of fringes, the uncertainty of the given densities is estimated to be about ±15%.

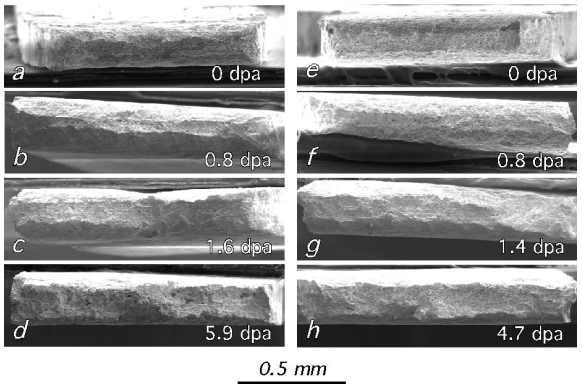

Fig. 3. SEM micrographs showing fracture surfaces of the samples of F82H, (a) to (d), and Optimax-A, (e) to (h), at different doses.

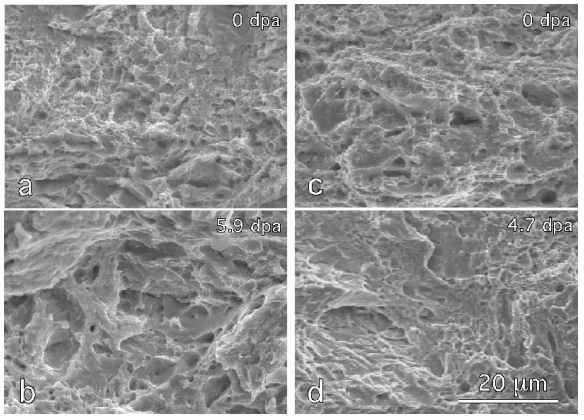

Fig. 4. SEM micrographs showing the ductile fracture in: (a) unirradiated, and (b) 5.9 dpa F82H samples; (c) unirradiated, and (d) 4.7 dpa Optimax-A samples.

4. Discussion

Three kinds of martensitic/ferritic steels, DIN1.4926 (10.5% Cr), F82H and Optimax-A, have been investigated after irradiation with 800-MeV protons at low temperatures, $\leqslant 230$°C. In general, both F82H and Optimax-A have very similar tensile properties as those measured for DIN 1.4926 [8,9], namely, radiation hardening increases continuously with irradiation dose up to about the same level of 6 dpa and uniform elongation drops to 1–2% starting at as little as 0.5 dpa. To compare radiation-hardening effects in these materials, the increase of yield stress after irradiation ($\Delta\sigma_{0.2}$) is plotted vs irradiation dose in Fig. 7. It can be seen that F82H has a lower radiation hardening than the other two kinds of materials. There is no significant difference between Optimax-A and DIN1.4926. It is also interesting to note that $\Delta\sigma_{0.2}$ is proportional to $(\text{dose})^{1/3}$ and does not show any saturation in the present dose range.

The present results are not sufficient to judge the usefulness of these materials for the application in spallation target windows which will receive up to 100 dpa per year. This is not only because the present irradiation-dose range is too low but also due to phenomena that are not yet understood. For example, on one hand, the materials show significant irradiation embrittlement effects indicated by very little uniform elongation, 1–2%, after irradiation. But on the other hand, the samples broke essentially in a ductile-fracture mode. In addition, the cross-section reduction remains above 40% at 5.9 dpa and even a little greater than that of unirradiated samples at a dose of 0.8 dpa.

The TEM results presented above describe essentially the same features observed in the previous work [8,9]: the size and density of defect clusters increase with irradiation dose and the precipitates become amorphous after irradiation. The small difference is that in

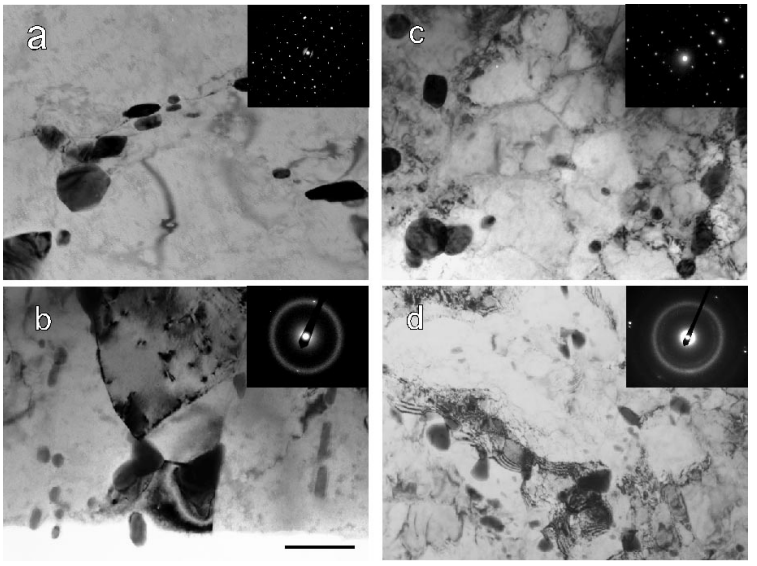

Fig. 5. TEM micrographs showing the precipitate structure in: (a) unirradiated, and (b) 0.8 dpa F82H samples; (c) unirradiated, and (d) 4.7 dpa Optimax-A samples. The diffraction patterns from large precipitates are inset which show that the precipitates change from a crystalline structure to amorphous after irradiation. The scale in (b) represents 250 nm for (a) and (b) and 500 nm for (c) and (d).

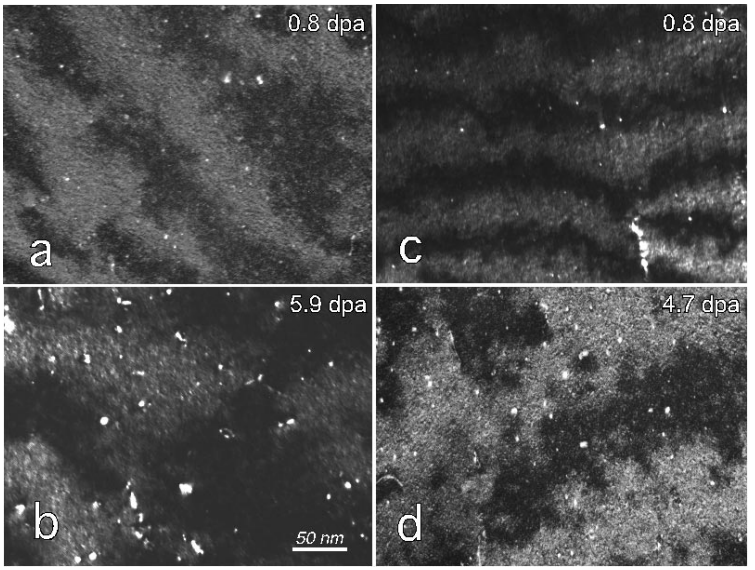

Fig. 6. WBDF micrographs showing the defect clusters in (a) 0.8 dpa and (b) 5.9 dpa F82H samples; (c) 0.8 dpa and (d) 4.7 dpa Optimax-A samples. The thickness at the central area is 30 nm for (a), (b) and (c), and 25 nm for (d).

DIN1.4926 [9], both defect-cluster size and density are much larger at the 6-dpa level as compared to those in F82H. In the F82H samples at 5.9 dpa, there are very few large loops (>10 nm) observed. In DIN1.4926, the large loops are already at high density. The reason for this difference is not clear yet. One possible reason can be that the irradiation temperature for the high dose DIN1.4926 samples may be about 100 K higher, i.e. around 200°C.

Radiation hardening is usually attributed to the defect clusters induced by irradiation. That F82H has lesser radiation hardening than DIN1.4926 can be explained with this argument because both the defect-cluster size and density in DIN1.4926 are greater.

Table 1
Defect cluster size and density in the irradiated F82H and Optimax-A samples

Material	Dose (dpa)	Mean cluster size (nm)	Cluster density (10^{22} m^{-3})
F82H	0.8	2.1	1.6
	1.6	2.4	2.2
	5.9	3.1	3.3
Optimax-A	0.8	2.2	2.0
	1.4	2.4	2.9
	4.7	3.0	3.0

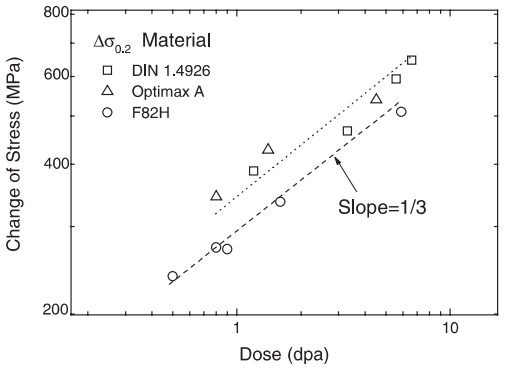

Fig. 7. Plot of the change of yield stress ($\Delta\sigma_{0.2}$) after irradiation vs irradiation dose. The results from [7] on DIN1.4926 martensitic steel (containing 10.5% Cr) are included for comparison.

However, the numbers in Table 1 indicate that F82H and Optimax-A have very similar defect-cluster size and density at similar doses. This makes it difficult to understand why F82H has less radiation hardening than Optimax-A. Whether there are other mechanisms, e.g. helium effects, since there is up to about 500 appm He in the 5.9 dpa sample, that contribute to hardening must be investigated.

5. Conclusion

Miniature tensile specimens were irradiated with 800-MeV protons at low temperature to 5.9 dpa. The preliminary investigations show that:

1. Irradiation hardening increases continuously with irradiation dose. The change in the yield stress is roughly proportional to $(\text{dose})^{1/3}$. F82H has lesser irradiation hardening than Optimax-A in the present work and lesser than DIN1.4926 from a previous study.
2. Uniform elongation is reduced sharply to less than 2% even at the lowest dose of 0.5 dpa. However, all the irradiated samples ruptured in a ductile mode.
3. TEM analyses have revealed that the size and density of defect clusters increase with irradiation dose. Precipitates become amorphous after irradiation.

Acknowledgements

The authors would like to thank Mr R. Brütsch at the Paul Scherrer Institute (PSI) for his help on SEM observation, Dr M. James and Dr P.D. Ferguson at Los Alamos National Laboratary (LANL) for calculating irradiation dose, to acknowledge M. Lopez, T. Romero, G. Willcutt at LANL and H. Kaiser and Mr X. Jia at PSI for their kind help on the experiment.

References

[1] K.Q. Bagley, E.A. Little, V. Levy, A. Alamo, K. Ehrlich, K. Anderko, A. Calza Bini, Nucl. Energy 27 (1988) 295.
[2] R.L. Klueh, D.J. Alexander, P.J. Maziasz, J. Nucl. Mater. 186 (1992) 185.
[3] M. Rieth, B. Dafferner, H.D. Röhrig, J. Nucl. Mater. 258–263 (1998) 1147.
[4] S.A. Maloy, W.F. Sommer, in: Proceedings of the Third International Workshop on Spallation Materials Science and Technology, Ancona, Italy, 1997, p. 297.
[5] Y. Dai, in: Proceedings of the Third International Workshop on Spallation Materials Science and Technology, Ancona, Italy, 1997, p. 265.
[6] A. Hishinuma, Y. Takagi, in: IEA Group Meeting on Ferritic Steels, Sun Valley, Idaho, June 1994.
[7] M. Victoria, E. Batawi, Ch. Briguet, D. Gavillet, P. Marmy, J. Paters, F. Rezai-Aria (to be published).
[8] Y. Dai, G.S. Bauer, F. Carsughi, H. Ullmaier, S.A. Maloy, W.F. Sommer, J. Nucl. Mater. 265 (1999) 203.
[9] Y. Dai, F. Carsughi, W.F. Sommer, G.S. Bauer, H. Ullmaier, J. Nucl. Mater. 276 (2000) 289.